Inorganic Chemistry

Article

pubs.acs.org/IC

Syntheses, Crystal Structures, Resistivity Studies, and Electronic Properties of Three New Barium Actinide Tellurides: $BaThTe_4$, $BaUTe_4$, and $BaUTe_6$

Jai Prakash,[†] Sébastien Lebègue,[‡] Christos D. Malliakas,[†] and James A. Ibers*[,†]

[†]Department of Chemistry, Northwestern University, 2145 Sheridan Road, Evanston, Illinois 60208-3113, United States

[‡]Laboratoire de Cristallographie, Résonance Magnétique et Modélisations (CRM2, UMR CNRS 7036), Institut Jean Barriol, Université de Lorraine, BP 239, Boulevard des Aiguillettes, 54506 Vandoeuvre-lès-Nancy, France

Supporting Information

ABSTRACT: The three new solid-state compounds $BaThTe_4$, $BaUTe_4$, and $BaUTe_6$ have been synthesized and characterized. $BaThTe_4$ and $BaUTe_4$ are isostructural. The structure consists of infinite $^2_\infty[AnTe_4^{2-}]$ layers separated by Ba^{2+} ions. Each An (An = Th, U) atom is coordinated to eight Te atoms in a bicapped trigonal-prismatic arrangement. Te atoms are connected to each other to form linear infinite chains. These Te−Te interactions are longer than that of a Te−Te single bond. However, this structure also possesses Te−Te single bonds. Charge balance in the formula $BaAnTe_4$ may be achieved with $[Ba^{2+}]_2[(An^{4+})_2(Te^{2-})_2(Te_2^{2-})(Te_2^{3-})_2]^{4-}$. The structure of $BaUTe_6$ features one-dimensional anionic $^1_\infty[UTe_6^{2-}]$ chains that are separated by Ba^{2+} ions. There are three Te−Te single bonds around each U atom. The anion in this structure can thus be described as $[U^{4+}(Te_2^{2-})_3]^{2-}$. Resistivity measurements on single crystals of $BaThTe_4$ and $BaUTe_6$ show semiconducting behavior. DFT calculations indicate finite band gaps for $BaThTe_4$ and for $BaUTe_6$, whereas $BaUTe_4$ has a vanishing density of states at the Fermi level.

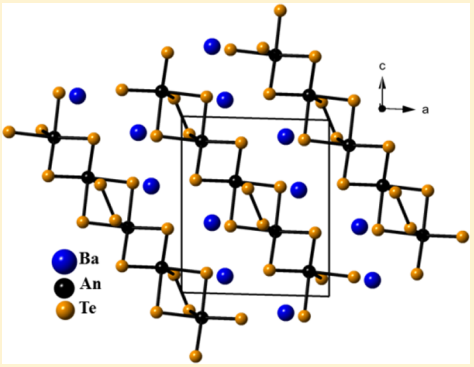

INTRODUCTION

Exploratory synthesis plays a vital role in the discovery of new actinide chalcogenides. These compounds show a variety of structural features as well as interesting magnetic,[1−3] optical,[1−3] and electronic properties, such as superconductivity[4,5] and charge density waves.[6] The tendency of the chalcogens (Q = S, Se, or Te) to form Q−Q bonds strongly affects the structures and properties of the actinide chalcogenides (An/Q). This is especially true of the tellurides where a wide range of Te−Te interactions exist that fall between a single Te−Te bond length (2.76 Å) and a Te−Te van der Waals interaction (≈4.10 Å). An example with single Te−Te bonds is the layered structure of α-UTe_3 (Te−Te = 2.751(1) Å).[7] On the basis of its structure this compound may be charge balanced as $U^{4+}Te^{2-}Te_2^{2-}$. In contrast, its polymorph β-UTe_3[8] possesses infinite layers comprising Te centers in square-planar coordination (Te···Te ≈ 3.01 Å), a configuration that is unstable on theoretical grounds.[9] There is no unambiguous way to charge balance β-UTe_3.

There are many examples of actinide telluride structures in which there are infinite Te−Te−Te−Te chains with intermediate Te−Te interactions. Such interactions often result in new structure types and complex crystal structures. Examples include the crystal structures of $CsAn_2Te_6$ (An = Th[10] and U[11]) and KTh_2Te_6[12] where the Te−Te distances range from 2.99 to 3.08 Å and where one manner of achieving charge balance is to assign −1.25 e^- to each Te in the chain. Clearly, such compounds are difficult to describe on the basis of simple bonding concepts, and the formulas do not readily charge balance. On the other hand, not all actinide tellurides have Te−Te interactions, and their formulas are readily charge-balanced. Examples include $MgThTe_3$,[13] A_2UTe_3 (A= K, Rb),[14] and BaU_2Te_5.[15]

Here we have turned to the Ak/An/Te system (Ak = alkaline-earth metal; An = Th, U) in the search for new compounds, an area that has been barely explored. Our exploratory syntheses have resulted in the discovery of the three new compounds $BaThTe_4$, $BaUTe_4$, and $BaUTe_6$. On the basis of their structures the first two do not readily charge balance whereas $BaUTe_6$ does. Here we present their syntheses, crystal structures, resistivities, and electronic properties.

EXPERIMENTAL METHODS

Syntheses and Analyses. *Caution!* *^{232}Th and depleted U are α-emitting radioisotopes and as such are considered a health risk. Their use requires appropriate infrastructure and personnel trained in the handling of radioactive materials.*

The following reactants were used for the syntheses of $BaThTe_4$, $BaUTe_4$, and $BaUTe_6$: U powder obtained by hydridization and decomposition of depleted U turnings (IBI Laboratories) in a

Received: September 14, 2014
Published: November 11, 2014

   dx.doi.org/10.1021/ic502246p | Inorg. Chem. 2014, 53, 12610−12616

modification[16] of a previous literature method,[17] Ba (Johnson Matthey, 99.5%), Th (MP Biomedicals, 99.1%), and Te (Aldrich, 99.8%). The reactions were performed in sealed carbon-coated fused-silica tubes. Chemical manipulations were performed inside an Ar-filled drybox. Reactants were weighed and transferred into the tubes that were then evacuated to 10^{-4} Torr, flame-sealed, and placed in a computer-controlled furnace. Semiquantitative analysis of the products was performed with an EDX-equipped Hitachi S-3400 SEM.

$BaThTe_4$. Black needles of $BaThTe_4$ were obtained from the reaction of Ba (23.7 mg, 0.172 mmol), Th (20 mg, 0.086 mmol), and Te (77 mg, 0.603 mmol). The reaction mixture was heated to 1023 K in 36 h, held there for 24 h, ramped to 1223 K, and annealed for 96 h. The reaction mixture was then cooled at 5 K/h to 298 K. The reaction product contained needles of $BaThTe_4$ (Ba:Th:Te ≈ 1:1:4), ThOTe (black plates),[18] and crystals of BaTe (Ba:Te ≈ 1:1).

$BaUTe_4$. Black needles of $BaUTe_4$ were obtained from the reaction of Ba (19.2 mg, 0.140 mmol), U (17 mg, 0.071 mmol), and Te (62.5 mg, 0.490 mmol). The reaction mixture was heated to 1023 K in 36 h, held there for 24 h, ramped to 1073 K, and annealed for 4 d. The reaction mixture was then cooled to 298 at 5 K/h. The reaction product contained black needles of $BaUTe_4$ and UOTe,[19] and crystals of BaTe. The black needles showed Ba:U:Te ≈ 1:1:4.

$BaUTe_6$. Black needles of $BaUTe_6$ were obtained from the reaction of Ba (20.8 mg, 0.151 mmol), U (30 mg, 0.126 mmol), and Te (101.3 mg, 0.794 mmol). The heating regime was the same as for $BaUTe_4$. The reaction product contained black needles of $BaUTe_6$ and UOTe,[19] and crystals of BaTe. The black needles showed Ba:U:Te ≈ 1:1:6.

Structure Determinations. Single-crystal X-ray diffraction data for $BaThTe_4$, $BaUTe_4$, and $BaUTe_6$ were collected on a Bruker APEX2 diffractometer with the use of graphite-monochromatized Mo Kα radiation (λ = 0.710 73 Å) at 100 K.[20] The algorithm COSMO in the program APEX2 was employed for the data collection strategy as a series of 0.3° scans in ω and φ. The exposure time was 10 s/frame, and the crystal-to-detector distance was 60 mm. The collection of the X-ray diffraction intensity data as well as cell refinement and data reduction were carried out with the use of the program APEX2.[20] Precession images of the three data sets did not show any evidence for modulation or super cells. Crystal structures of all three compounds were solved by direct methods and refined with the use of the SHELX14 program package.[21,22] The program SADABS was used for face-indexed absorption, incident beam, and decay corrections.[22] The atomic positions were standardized using the program STRUCTURE TIDY[23] in PLATON.[24] Further crystallographic details are given in Table 1 and in the Supporting Information.

Resistivity Studies. Four-probe high-temperature-dependent resistivity data were collected using a homemade resistivity apparatus equipped with a Keithley 2182 nanovoltmeter, a Keithley 236 source measure unit, and a high-temperature vacuum chamber controlled by a K-20 MMR system. An $I-V$ curve from 1×10^{-5} A to -1×10^{-5} A with a step of 2×10^{-6} A was measured for each temperature point (from 300 to 450 K), and resistance was calculated from the slope of the $I-V$ plot. Data acquisition was controlled by custom-written software. Graphite paint (PELCO isopropanol-based graphite paint) was used for electrical contacts with Cu wire of 0.025 mm thickness (Omega). The dc current was applied along an arbitrary direction.

Theoretical Calculations. The ab initio calculations have been performed using the VASP (Vienna ab Initio Simulation Package) code,[25,26] implementing density functional theory[27,28] in the framework of the projector augmented wave (PAW) method.[29] By combining plane waves and local orbitals the PAW method obtains the correct shape of the wave function near the atomic nuclei. We have used the Heyd, Scuseria, Ernzerhof (HSE) functional[30,31] for the exchange-correlation, allowing for spin-polarization of the electron density. For each structure the geometry used was the experimental one. The different possible magnetic orders that can occur in the crystal unit cell were calculated; the one with the lowest total energy was retained as the ground state. To reach convergence, we have used the default cutoff for the wave function and a k-point mesh of 4 × 6 × 4 for $BaThTe_4$ and $BaUTe_4$ and 4 × 2 × 4 for $BaUTe_6$ to sample the Brillouin zone.

Table 1. Crystallographic Data for $BaThTe_4$, $BaUTe_4$, and $BaUTe_6$[a]

	$BaThTe_4$	$BaUTe_4$	$BaUTe_6$
space group	C_{2h}^3–$I2/m$	C_{2h}^3–$I2/m$	C_{sh}^3–$P2_1/c$
a (Å)	10.460 (2)	10.363 (2)	8.8483 (3)
b (Å)	6.3800 (13)	6.3037(13)	15.0414 (4)
c (Å)	12.580 (3)	12.458 (2)	8.0855 (2)
β (deg)	91.54 (3)	91.26 (3)	91.424 (2)
V (Å^3)	839.2 (3)	813.6 (3)	1075.77 (5)
ρ (g cm^{-3})	6.963	7.231	7.045
μ (mm^{-1})	35.89	38.64	34.55
$R(F)^b$	0.027	0.024	0.031
$R_w(F_o^2)^c$	0.074	0.060	0.061

[a]For all structures, λ = 0.710 73 Å, T = 100(2) K, and Z = 4. [b]$R(F) = \Sigma||F_o| - |F_c||/\Sigma|F_o|$ for $F_o^2 > 2\sigma(F_o^2)$. [c]$R_w(F_o^2) = \{\Sigma[w(F_o^2 - F_c^2)^2]/\Sigma wF_o^4\}^{1/2}$. For $F_o^2 < 0$, $w^{-1} = \sigma^2(F_o^2)$; for $F_o^2 \geq 0$, $w^{-1} = \sigma^2(F_o^2) + (qF_o^2)^2$ where q = 0.0217 for $BaThTe_4$, 0.0100 for $BaUTe_4$, and 0.0167 for $BaUTe_6$.

RESULTS AND DISCUSSION

Syntheses. The compound $BaThTe_4$ was obtained in a yield of about 30 wt % based on Th by the reaction of the elements at 1223 K. Other secondary phases were ThOTe and BaTe. Further attempts to improve the yield of this compound by loading stoichiometric amounts of Ba, Th, and Te failed. The compounds $BaUTe_4$ and $BaUTe_6$ were obtained in yields of about 30 and 20 wt %, respectively, based on U by reactions of the elements at 1073 K. Other secondary phases were UOTe and BaTe. No attempt was made to maximize the yields for these two compounds.

Crystal Structures of $BaThTe_4$ and $BaUTe_4$. These isostructural compounds crystallize in a new structure type in the space group C_{2h}^3–$I2/m$ of the monoclinic system. There are four formula units in the unit cell. The asymmetric unit comprises An1(site symmetry m), Ba1(m), Te1(1), Te2(m), and Te3(m). The reduction in cell volume in going from $BaThTe_4$ to $BaUTe_4$ of 839.2(3) Å^3 to 813.6(3) Å^3 (Table 1) is the result of the actinide contraction.

The structure consists of infinite $^2_\infty[AnTe_4^{2-}]$ layers separated by Ba^{2+} ions (Figure 1). Important interatomic

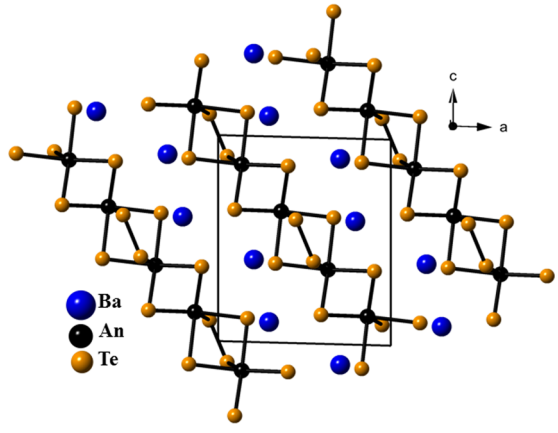

Figure 1. Crystal structure of the $BaAnTe_4$ (An = Th and U) compounds viewed along [010].

dx.doi.org/10.1021/ic502246p | Inorg. Chem. 2014, 53, 12610−12616

distances are given in Table 2. Each An atom is coordinated to eight Te atoms in a bicapped trigonal-prismatic arrangement

Table 2. Selected Interatomic Distances (Å) in $BaThTe_4$, $BaUTe_4$, and $BaUTe_6$

	$BaThTe_4$	$BaUTe_4$	$BaUTe_6$
An1−Te1	3.2177(7) × 2	3.1629(7) × 2	3.1678 (6)
An1−Te1	3.2347(7) × 2	3.1632(7) × 2	3.1711 (6)
An1−Te2	3.3495(6) × 2	3.3047(6) × 2	3.1195 (6)
An1−Te3	3.1989(9)	3.1449 (9)	3.1295(6)
An1−Te3	3.2105(9)	3.1450 (9)	
An1−Te4			3.1617(6)
An1−Te4			3.1794(6)
An1−Te5			3.1593(6)
An1−Te5			3.1807(6)
An1−Te6			3.1086(6)
Te1···Te1	3.1857(11)	3.1506(10)	
Te1···Te1	3.1943(11)	3.1531(10)	
Te2−Te2	2.7661(12)	2.7590(12)	
Te1−Te2			2.8158(7)
Te3−Te4			2.8351(7)
Te5−Te6			2.8526(7)
An···An	4.5530(1)	4.5220(1)	4.0428(1)

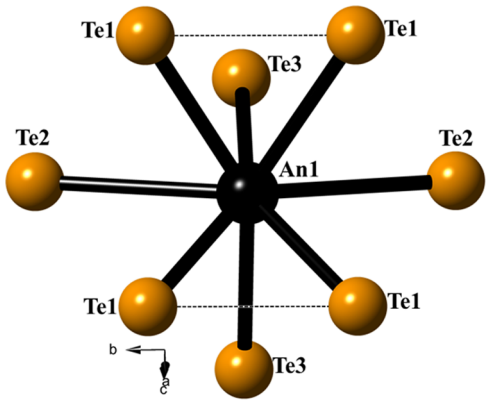

Figure 2. Local coordination environment of the An atom in the crystal structure of $BaAnTe_4$ (An = Th and U). Te1−Te1 interactions are shown by dashed lines.

(Figure 2). The An−Te distances range from 3.1989(9) to 3.3495(6) Å (An = Th) and 3.1449(9) to 3.3047(6) Å (An = U). Te1 atoms are connected to each other to form linear infinite chains that run along the *b*-axis. The Te1−Te1 interactions are 3.1857(11) and 3.1943(11) Å for $BaThTe_4$ and 3.1506(10) and 3.1531(10) Å for $BaUTe_4$. Te2 atoms connect two An1 atoms in the *b*-direction, while two Te3 atoms bridge between two An1 atoms along the $[10\bar{1}]$ direction (Figure 3). In addition to infinite Te1−Te1 chains, this structure also possesses Te2−Te2 single bonds with distances of 2.7661(12) Å (An = Th) and 2.7590(12) Å (An = U). The various An−Te and Te−Te single bonds and interactions are normal as compared with those in related compounds (Tables 3 and 4). Barium atoms in $BaAnTe_4$ are coordinated to nine Te atoms in a tricapped trigonal-prismatic fashion (Figure 4). Ba−Te distances range from 3.4545(7) to 3.6316(9) Å (An = Th) and 3.4334(7) to 3.6136(11) Å (An = U). The latter may be

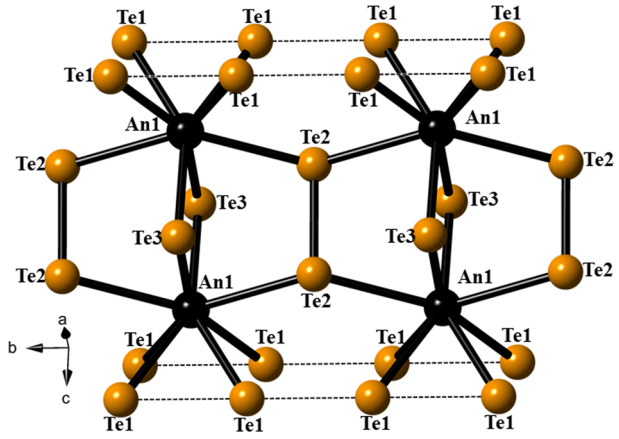

Figure 3. An network in $BaAnTe_4$ (An = Th and U).

Table 3. Th−Te and Te−Te Interactions in Known Thorium Tellurides[a]

compd	structure	Th−Te (Å)	Te−Te (Å)	ref
α-$ThTe_3$	layered	3.171(1)−3.250(1)	2.763(1)	35
Th_7Te_{12}	3-dimensional	3.137(2)−3.483(1)		36
$CuTh_2Te_6$	3-dimensional	3.165(1)−3.273(1)	3.058(1), 3.113(1)	37
KTh_2Te_6	layered	3.166(2)−3.264(1)	3.057(3), 3.085(3)	12
$CsTh_2Te_6$	layered	3.164(2)−3.264(2)	3.052(3), 3.088(3)	10
$MnThTe_3$	3-dimensional	3.160(1)−3.374(1)		13
$MgThTe_3$	3-dimensional	3.157(1)−3.374(1)		13

[a]Some entries have been rounded to three significant figures to facilitate comparisons.

compared with the Ba−Te distances in BaU_2Te_5 of 3.574(1) to 3.641(1) Å.[15]

Because of the presence of the infinite Te−Te−Te chains of intermediate length in $BaThTe_4$ and $BaUTe_4$ the assignment of formal oxidation states is somewhat arbitrary. One such assignment is to place an average charge of −1.5 e^- on the Te atoms in the infinite chains. Then charge balance in the formula $BaAnTe_4$ may be achieved with $[Ba^{2+}]_2[(An^{4+})_2(Te^{2-})_2(Te_2^{2-})(Te_2^{3-})_2]^{4-}$. Noninteger charge on Te atoms in such infinite Te chains has been discussed for a variety of actinide tellurides including Cu_xUTe_3[32] and $ATiU_3Te_9$ (A = Rb and Cs).[33]

Crystal Structure of $BaUTe_6$. This compound crystallizes in a new structure type in space group C_{5h}^3−$P2_1/c$ of the monoclinic system (Table 1). There are four formula units in the cell. The asymmetric unit of the structure comprises one U, one Ba, and six Te atoms all in general positions. The crystal structure features one-dimensional anionic $^1_\infty[UTe_6^{2-}]$ chains along [001] that are separated by Ba^{2+} ions (Figure 5a). Crystallographic details and important interatomic distances are given in Tables 1 and 2, respectively. Each U atom is coordinated to nine Te atoms in a tricapped trigonal-prismatic arrangement (Figure 6). Each U atom is connected to a neighboring U atom by the sharing of the Te1/Te4/Te5 triangular face (Figure 7). There are three Te−Te single bonds around each U atom (Table 2). The anion in this structure can thus be described as $[U^{4+}(Te_2^{2-})_3]^{2-}$. The U−Te interatomic distances are comparable with those in related uranium tellurides (Table 4). The Ba atom in $BaUTe_6$ is coordinated

dx.doi.org/10.1021/ic502246p | Inorg. Chem. 2014, 53, 12610−12616

Table 4. U−Te and Te−Te Interactions in Known Uranium Tellurides[a]

compd	structure	U−Te distances (Å)	Te−Te (Å)	ref
$BaUTe_4$	layered	3.145(1)−3.305(1)	2.759(1)-3.153(1)	this work
$BaUTe_6$	1-dimensional	3.109(1)−3.181(1)	2.816(1)-2.853(1)	this work
UTe_2	3-dimensional	3.080(1)−3.203(1)		38
α-UTe_3	layered	3.103(1)−3.205(1)	2.751(1)	7
β-UTe_3	layered	3.192(3)−3.201(1)	3.067(1)	8
$CsUTe_6$	1-dimensional	3.006(8)−3.265(7)	2.791(6)-3.175(5)	34
CsU_2Te_6	layered	3.089(1)−3.203(1)	2.989(1), 3.049(1)	11
$Cu_{0.78}U_2Te_6$	layered	3.100(1)−3.236(1)	3.028(1), 3.073(1)	39
$Tl_{0.56}UTe_3$	layered	3.093(2)−3.225(1)	3.037(3), 3.054(3)	40
BaU_2Te_5	layered	3.063(1)−3.219(1)		15
$CsZrUTe_5$	layered	3.096(1)−3.360(1)	3.155(1)	41
$CsTiUTe_5$	layered	3.059(1)−3.262(1)	3.065(1)	34
$CsTiU_3Te_9$	3-dimensional	2.966(3)−3.276(3)	3.051(1)−3.064(1)	33
$RbTiU_3Te_9$	3-dimensional	3.000(1)−3.216(1)	3.046(1)−3.051(1)	33
$Cs_8Hf_5UTe_{30.6}$	1-dimensional	3.018(3)−3.189(3)	2.714(8)−3.066(4)	34

[a]Some entries have been rounded to three significant figures to facilitate comparisons.

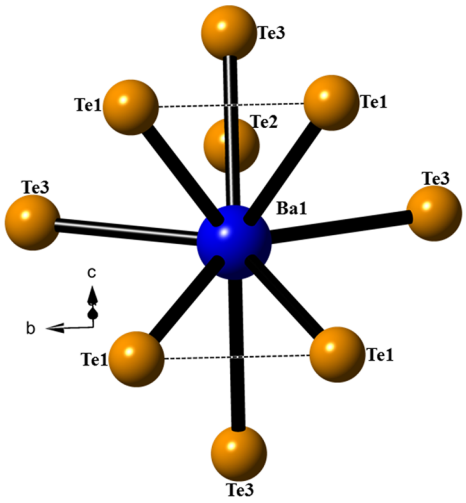

Figure 4. Coordination environment of the Ba atom in the $BaAnTe_4$ (An = Th and U) structures.

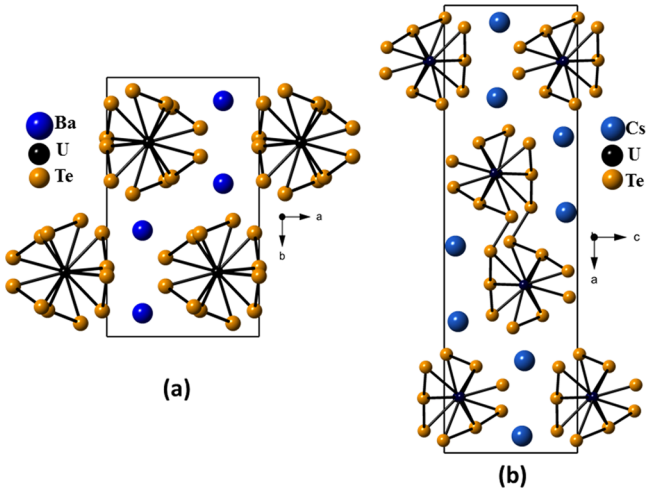

Figure 5. Comparison of the structures of (a) $BaUTe_6$ and (b) $CsUTe_6$.[34]

to nine Te atoms (Figure 8) with Ba−Te distances ranging from 3.4927(7) to 3.8195(7) Å.

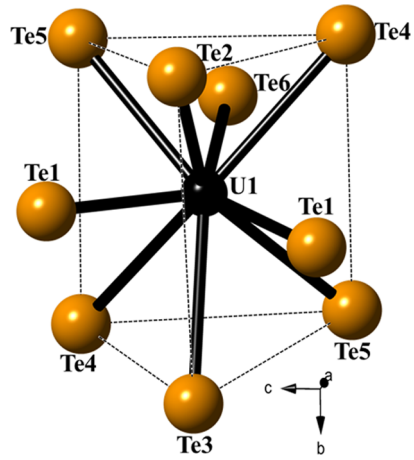

Figure 6. Local coordination environment of the U atom in the crystal structure of $BaUTe_6$. The dashed lines serve to aid visualization of the tricapped trigonal-prismatic coordination of the U atom.

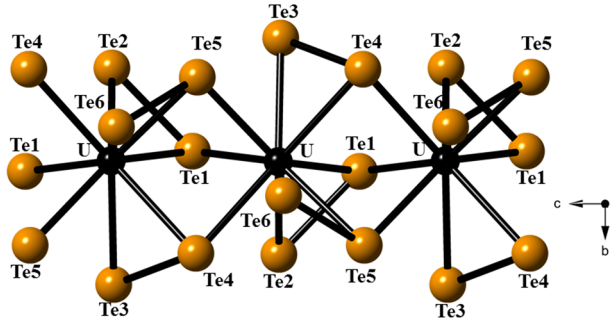

Figure 7. Infinite U chains viewed along [100] in the structure of $BaUTe_6$.

The crystal structure of $BaUTe_6$ shows some resemblance to another "116" compound, namely $CsUTe_6$[34] (Figure 5b), that also features one-dimensional U/Te chains. However, in the structure of $CsUTe_6$, two one-dimensional U/Te chains interact with each other through Te−Te contacts. These interactions are missing in the structure of $BaUTe_6$.

Resistivity Studies. High-temperature-dependent resistivity data on single crystals of $BaThTe_4$ and $BaUTe_6$ show decreasing resistivity with increasing temperature indicative of

dx.doi.org/10.1021/ic502246p | Inorg. Chem. 2014, 53, 12610−12616

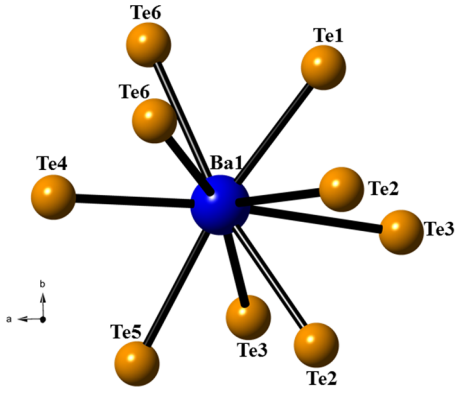

Figure 8. Coordination environment of the Ba atom in the $BaUTe_6$ structure.

semiconducting behavior (Figure 9). $BaThTe_4$ is the most resistive member with resistivity of 5.3 MΩ cm at 298 K and 1.1

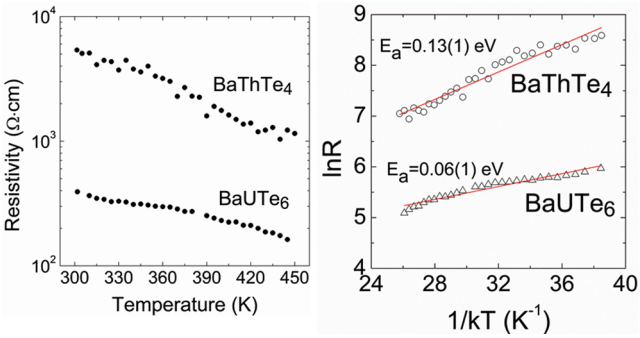

Figure 9. Resistivities and their corresponding Arrhenius plots for single crystals of $BaThTe_4$ and $BaUTe_6$.

MΩ cm at 450 K. $BaUTe_6$ has a resistivity of about 390 Ω cm at 298 K and 160 Ω cm at 450 K. The calculated activation energies are 0.13(1) eV for $BaThTe_4$ and 0.06(1) eV for $BaUTe_6$.

Electronic Structures. $BaThTe_4$ is not magnetic, and from the calculated total density of states (see upper plot of Figure 10) it has a finite band gap of approximately 0.6 eV. Therefore, the semiconducting character as found experimentally is confirmed. From the various partial density of states for each nonequivalent atom it can be seen that the top of the valence bands corresponds mainly to Te1-p and Th-f states, whereas the bottom of the conduction bands consists mainly of Te2-p, Th-f, and Th-d states. The strong hybridization of the Th atom with the Te1 atom is seen from the states immediately below the Fermi level that share a similar shape as a function of energy. The same structure with a weaker intensity is also found in the density of states of atoms Te2, Te3, and Ba. In contrast, $BaUTe_4$ is found to be antiferromagnetic, as illustrated by its spin-polarized density of states (Figure 11). At the Fermi level, the density of states is very small, so $BaUTe_4$ is a poor metal. Also, the finite magnetic moment on the U atoms induces a small magnetic polarization on the other atoms, as seen from their partial density of states that are not symmetric with respect to the spin. Also, $BaUTe_6$ is found to be ferromagnetic with a gap of 1.4 eV (see upper plot of Figure 12), which is in agreement with the resistivity measurement. The top of the valence states and the bottom of the conduction bands are both made from U-f and Te-p states.

We found that when using the generalized gradient approximation (GGA) instead of the HSE functional, the Fermi level of $BaUTe_6$ fell between two peaks of the density of states but with a finite value at the Fermi level. This highlights the importance of using the HSE functional for a correct description of the electronic structures of actinide compounds that have a band gap.

CONCLUSIONS

Exploratory syntheses have resulted in the discovery of the three new solid-state compounds $BaThTe_4$, $BaUTe_4$, and $BaUTe_6$. Each was synthesized in reasonable yields by standard high-temperature techniques. Their structures have been determined from single-crystal X-ray diffraction data. $BaThTe_4$ and $BaUTe_4$ are isostructural and crystallize in space group C_{2h}^3–$I2/m$ of the monoclinic system. The structure consists of infinite $^2_\infty[AnTe_4^{2-}]$ layers separated by Ba^{2+} ions. Each An atom is coordinated to eight Te atoms in a bicapped trigonal-prismatic arrangement. Te atoms are connected to each other to form linear infinite chains. These Te–Te interactions are longer than that of a Te–Te single bond. However, this

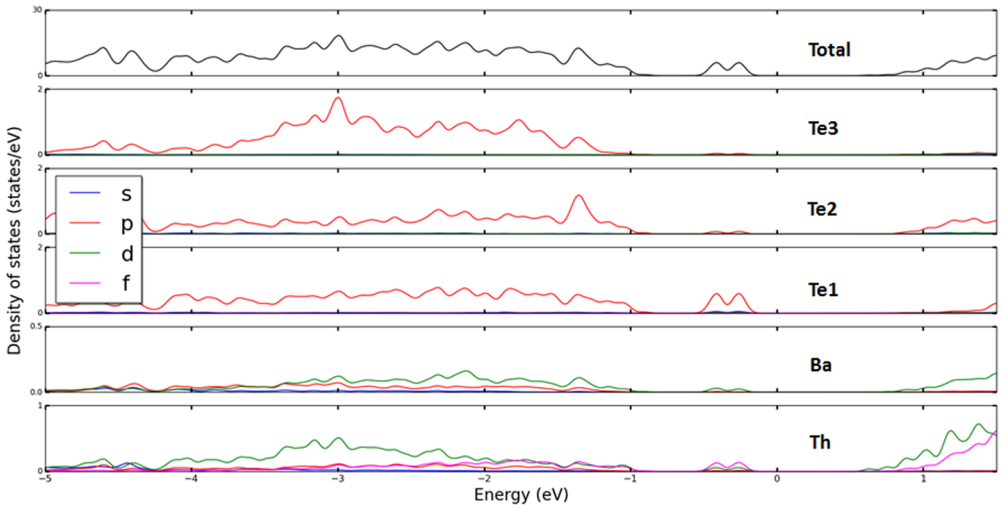

Figure 10. Calculated total (upper plot) and partial (lower plots) density of states for $BaThTe_4$.

dx.doi.org/10.1021/ic502246p | Inorg. Chem. 2014, 53, 12610–12616

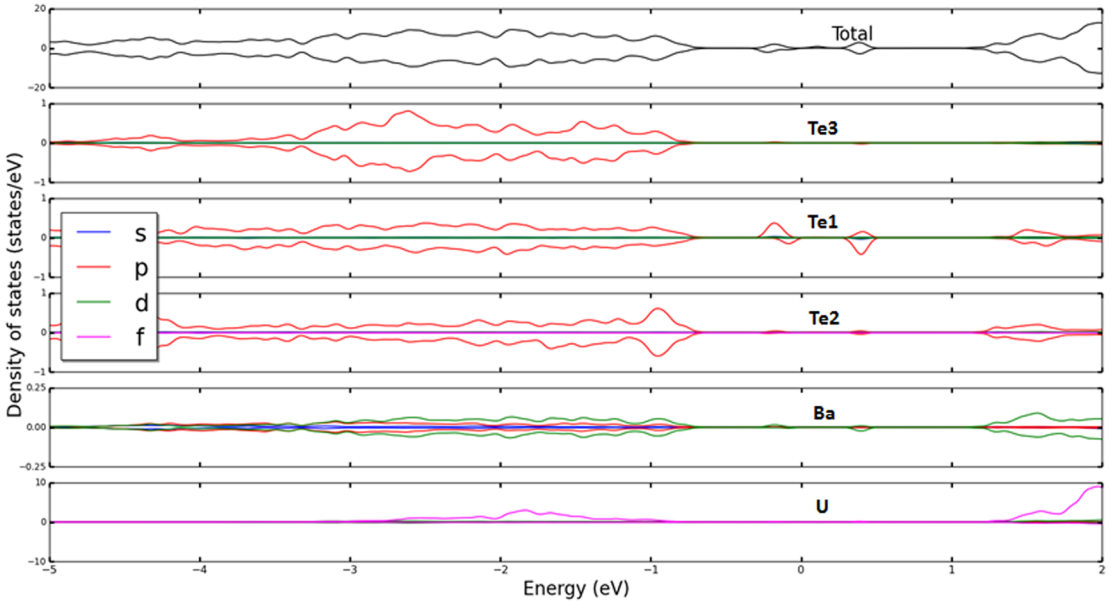

Figure 11. Calculated total (upper plot) and partial (lower plots) density of states for $BaUTe_4$.

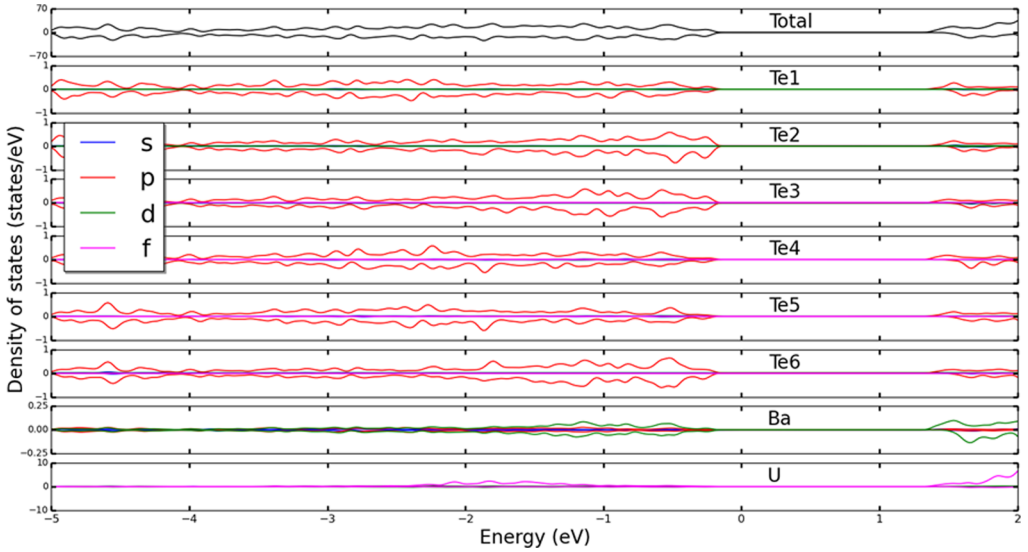

Figure 12. Calculated total (upper plot) and partial (lower plots) density of states for $BaUTe_6$.

structure also possesses Te−Te single bonds. The assignment of formal oxidation states in $BaThTe_4$ and $BaUTe_4$ is somewhat arbitrary owing to the presence of the infinite Te−Te−Te chains that possess distances intermediate between those of a normal single bond and a van der Waals interaction. However, on the assumption of Th^{4+}, charge balance in the formula $BaThTe_4$ may be achieved with $[Ba^{2+}]_2[(Th^{4+})_2(Te^{2-})_2(Te_2^{2-})(Te_2^{3-})_2]^{4-}$. $BaUTe_4$ may be charge balanced similarly.

$BaUTe_6$ crystallizes in a new structure type in space group C_{2h}^5−$P2_1/c$ of the monoclinic system. Its crystal structure features one-dimensional anionic $^1_\infty[UTe_6^{2-}]$ chains that are separated by Ba^{2+} ions. Each U atom is coordinated to nine Te atoms in a tricapped trigonal-prismatic arrangement. Each U atom is connected to neighboring U atoms by the sharing of Te/Te/Te triangular faces. There are three Te−Te single bonds around each U atom. The anion in this structure can thus be described as $[U^{4+}(Te_2)^{2-}{}_3]^{2-}$.

Resistivity measurements on single crystals of $BaThTe_4$ and $BaUTe_6$ show decreasing resistivity with increasing temperature indicative of semiconducting behavior.

Theoretical calculations have been performed using density functional theory with the HSE functional. $BaThTe_4$ is not magnetic, and from the calculated total density of states it has a finite band gap of approximately 0.6 eV; therefore, the semiconducting character of $BaThTe_4$, as found experimentally, is confirmed. $BaUTe_4$ is found to be antiferromagnetic, with a small value of the density of states at the Fermi level. Therefore, $BaUTe_4$ is a poor metal. Finally, $BaUTe_6$ is found to be ferromagnetic with a gap of 1.4 eV, which is consistent with the resistivity measurement showing semiconducting behavior.

dx.doi.org/10.1021/ic502246p | *Inorg. Chem.* 2014, 53, 12610−12616

■ ASSOCIATED CONTENT

Supporting Information

Crystallographic files in CIF format for $BaThTe_4$, $BaUTe_4$, and $BaUTe_6$. This material is available free of charge via the Internet at http://pubs.acs.org.

■ AUTHOR INFORMATION

Corresponding Author

*E-mail: ibers@chem.northwestern.edu.

Notes

The authors declare no competing financial interest.

■ ACKNOWLEDGMENTS

Use was made of the IMSERC X-ray Facility at Northwestern University, supported by the International Institute of Nanotechnology (IIN). S. L. acknowledges HPC resources from GENCI-CCRT/CINES (Grant x2014-085106).

■ REFERENCES

(1) *The Actinides: Electronic Structure and Related Properties*; Freeman, A. J., Darby, J. B., Jr., Eds.; Academic Press: New York, 1974; Vols. *1*−*2*.

(2) Bugaris, D. E.; Ibers, J. A. *Dalton Trans.* **2010**, *39*, 5949−5964.

(3) Manos, E.; Kanatzidis, M. G.; Ibers, J. A. In *The Chemistry of the Actinide and Transactinide Elements*, 4th ed.; Morss, L. R., Edelstein, N. M., Fuger, J., Eds.; Springer: Dordrecht, The Netherlands, 2010; Vol. *6*, pp 4005−4078.

(4) Damien, D.; de Novion, C. H.; Gal, J. *Solid State Commun.* **1981**, *38*, 437−440.

(5) de Novion, C. H.; Damien, D.; Hubert, H. *J. Solid State Chem.* **1981**, *39*, 360−367.

(6) Choi, K.-S.; Patschke, R.; Billinge, S. J. L.; Waner, M. J.; Dantus, M.; Kanatzidis, M. G. *J. Am. Chem. Soc.* **1998**, *120*, 10706−10714.

(7) Stöwe, K. *Z. Anorg. Allg. Chem.* **1996**, *622*, 1419−1422.

(8) Noël, H.; Levet, J. C. *J. Solid State Chem.* **1989**, *79*, 28−33.

(9) Tremel, W.; Hoffmann, R. *J. Am. Chem. Soc.* **1987**, *109*, 124−140.

(10) Cody, J. A.; Ibers, J. A. *Inorg. Chem.* **1996**, *35*, 3836−3838.

(11) Mesbah, A.; Ibers, J. A. *Acta Crystallogr., Sect. E: Struct. Rep. Online* **2012**, *68*, i76.

(12) Wu, E. J.; Pell, M. A.; Ibers, J. A. *J. Alloys Compd.* **1997**, *255*, 106−109.

(13) Narducci, A. A.; Ibers, J. A. *Inorg. Chem.* **2000**, *39*, 688−691.

(14) Stöwe, K.; Appel-Colbus, S. *Z. Anorg. Allg. Chem.* **1999**, *625*, 1647−1651.

(15) Prakash, J.; Tarasenko, M. S.; Mesbah, A.; Lebégue, S.; Malliakas, C.; Ibers, J. A. *Inorg. Chem.* **2014**, DOI: 10.1021/ic501795w.

(16) Bugaris, D. E.; Ibers, J. A. *J. Solid State Chem.* **2008**, *181*, 3189−3193.

(17) Haneveld, A. J. K.; Jellinek, F. *J. Less-Common Met.* **1969**, *18*, 123−129.

(18) Beck, H. P.; Dausch, W. *Z. Anorg. Allg. Chem.* **1989**, *571*, 162−164.

(19) Murasik, A.; Suski, W.; Leciejewicz, J. *Phys. Status Solidi* **1969**, *34*, K157−K158.

(20) *Bruker APEX2 Version 2009.5-1 Data Collection and Processing Software*; Bruker Analytical X-Ray Instruments, Inc.: Madison, WI, 2009.

(21) Sheldrick, G. M. *Acta Crystallogr., Sect. A: Found. Crystallogr.* **2008**, *64*, 112−122.

(22) Sheldrick, G. M. *SADABS*; Department of Structural Chemistry, University of Göttingen: Göttingen, Germany, 2008.

(23) Gelato, L. M.; Parthé, E. *J. Appl. Crystallogr.* **1987**, *20*, 139−143.

(24) Spek, A. L. *PLATON, A Multipurpose Crystallographic Tool*; Utrecht University: Utrecht, The Netherlands, 2014.

(25) Kresse, G.; Forthmüller, J. *Comput. Mater. Sci.* **1996**, *6*, 15−50.

(26) Kresse, G.; Joubert, D. *Phys. Rev. B* **1999**, *59*, 1758−1775.

(27) Hohenberg, P.; Kohn, W. *Phys. Rev.* **1964**, *136*, 864−871.

(28) Kohn, W.; Sham, L. J. *Phys. Rev.* **1965**, *140*, 1133−1138.

(29) Blöchl, P. E. *Phys. Rev. B* **1994**, *50*, 17953−17979.

(30) Heyd, J.; Scuseria, G. E.; Ernzerhot, M. *J. Chem. Phys.* **2006**, *124*, 219906-1.

(31) Heyd, J.; Scuseria, G. E.; Ernzerhof, M. *J. Chem. Phys.* **2003**, *118*, 8207−8215.

(32) Patschke, R.; Breshears, J. D.; Brazis, P.; Kannewurf, C. R.; Billinge, S. J. L.; Kanatzidis, M. G. *J. Am. Chem. Soc.* **2001**, *123*, 4755−4762.

(33) Ward, M. D.; Mesbah, A.; Lee, M.; Malliakas, C. D.; Choi, E. S.; Ibers, J. A. *Inorg. Chem.* **2014**, *53*, 7909−7915.

(34) Cody, J. A.; Ibers, J. A. *Inorg. Chem.* **1995**, *34*, 3165−3172.

(35) Prakash, J.; Ibers, J. A. *Z. Anorg. Allg. Chem.* **2014**, *640*, 1943−1945.

(36) Tougait, O.; Potel, M.; Noël, H. *Inorg. Chem.* **1998**, *37*, 5088−5091.

(37) Narducci, A. A.; Ibers, J. A. *Inorg. Chem.* **1998**, *37*, 3798−3801.

(38) Beck, H. P.; Dausch, W. *Z. Naturforsch., B: Chem. Sci.* **1988**, *43*, 1547−1550.

(39) Huang, F. Q.; Ibers, J. A. *J. Solid State Chem.* **2001**, *159*, 186−190.

(40) Tougait, O.; Daoudi, A.; Potel, M.; Noël, H. *Mater. Res. Bull.* **1997**, *32*, 1239−1245.

(41) Kim, J.-Y.; Gray, D. L.; Ibers, J. A. *Acta Crystallogr., Sect. E: Struct. Rep. Online* **2006**, *E62*, i124−i125.